JOURNAL OF CHEMICAL EDUCATION

pubs.acs.org/jchemeduc

Laboratory Experiment

Synthesis and Analysis of Zinc Copper Indium Sulfide Quantum Dot Nanoparticles

George Lisensky,* Ross McFarland-Porter, Weltha Paquin, and Kangying Liu

Cite This: https://dx.doi.org/10.1021/acs.jchemed.9b00642

Read Online

ACCESS | Metrics & More | Article Recommendations | Supporting Information

ABSTRACT: Nanoparticle $Zn_{2x}Cu_{1-x}In_{1-x}S_2$ is a promising and safer alternative to lead- and cadmium-containing quantum dots. Students prepare $Zn_{0.44}Cu_{0.78}In_{0.78}S_2$ quantum dots in a one-pot synthesis without an inert atmosphere and investigate how the color, visible absorption band edge, and photoluminescence peak wavelength depend on the size of the particle. Octadecene is used as a noncoordinating solvent with a high boiling point. Oleic acid and stearic acid are used as ligands to dissolve the metal salts in the solvent at ∼150 °C. Dodecanethiolate coordinates to the metal ion, and above 200 °C, the metal thiolate decomposes to produce metal sulfide nanoparticles, coated in dodecanethiolate. Samples are withdrawn from the hot solution and quenched at room temperature to produce a series of increasing nanoparticle sizes with the same chemical composition.

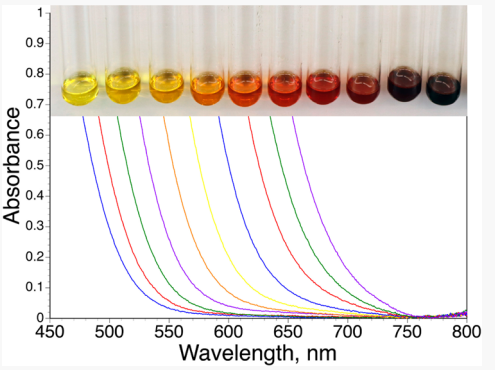

KEYWORDS: *Fluorescence Spectroscopy, Hands-On Learning/Manipulatives, Inorganic Chemistry, Laboratory Instruction, Nanotechnology, Upper-Division Undergraduate, UV−Vis Spectroscopy, Materials Science, Atomic Spectroscopy*

INTRODUCTION

A quantum dot (QD) is a semiconductor crystal with a diameter of a few nanometers and whose color, visible absorption wavelength, and photoluminescence peak wavelength are tunable by changing the particle size. This fundamental nanochemistry concept has been frequently illustrated in this *Journal*. Laboratory experiments using QDs have made use of CdSe,[1−5] CdS,[3,6−8] ZnO,[9,10] C,[11,12] PbS,[6,13] Cu_2O,[14] and $CsPbX_3$.[15] QDs are an intriguing material for applications in solar cells,[16,17] in video displays,[18] as hydrolysis photocatalysts,[19] in white LED lighting,[20] in photoluminescent labeling for bioimaging,[21] and for cancer treatment.[22] However, the toxicity[23] of Cd and Pb make many of these materials problematic for general use and prohibited for consumer goods in some countries.

CdSe QDs have been of interest because their band gap is well-matched to the visible spectrum so a full range of visible colors are available.[1] The QD wavelength ranges for ZnO[9,10] and ZnS[24] are in the ultraviolet portion of the spectrum. Zinc copper indium sulfide QDs incorporate less harmful elements;[25] their band gap matches the visible region of the electromagnetic spectrum, and zinc increases the photoluminescence intensity relative to $CuInS_2$,[17,20,26] making them a promising QD material.

Many QD synthesis procedures involve injecting a cooler solution of some of the reagents into a hot solution of the remaining reagents.[1,3,5,16,27] This method has the advantage of creating many nucleation sites to promote small particle sizes but the disadvantage of requiring rapid and homogeneous mixing. An alternative method, where decomposition of one component produces the limiting reactant,[13,20,25,28,29] requires rapid heating to again produce large numbers of nucleation sites in a short period of time. In this experiment, thermal decomposition of dodecanethiol serves as the sulfide source and allows for a one-pot synthesis. Many zinc copper indium sulfide syntheses use an inert atmosphere, but the synthesis reported here is done under ambient air. Nanoparticles generally need a surface ligand to prevent the particles from joining together and producing a bulk precipitate.[30] The dodecanethiol serves as the source of both the sulfur and the surface ligand.[31]

The sphalerite structure of cubic ZnS can be viewed as a derivative of the diamond structure with Zn and S alternating (Figure 1, left). The $CuInS_2$ chalcopyrite structure can be viewed as two stacked diamond unit cells, with interspersed Cu and In on the metal site (Figure 1, right). Mixing these two structures gives the $Zn_{2x}(CuIn)_{1-x}S_2$ family whose members exist as solid solutions for $2x > 0.41$.[31,32] In this solid solution two zinc atoms randomly replace a copper atom and an indium atom in the chalcopyrite structure as required by the charge balance for Zn^{2+}, Cu^+, and In^{3+}. A formula like $Zn_{0.44}Cu_{0.78}In_{0.78}S_2$ means that a given Cu or In site in the structure has a

Received: July 14, 2019
Revised: December 19, 2019

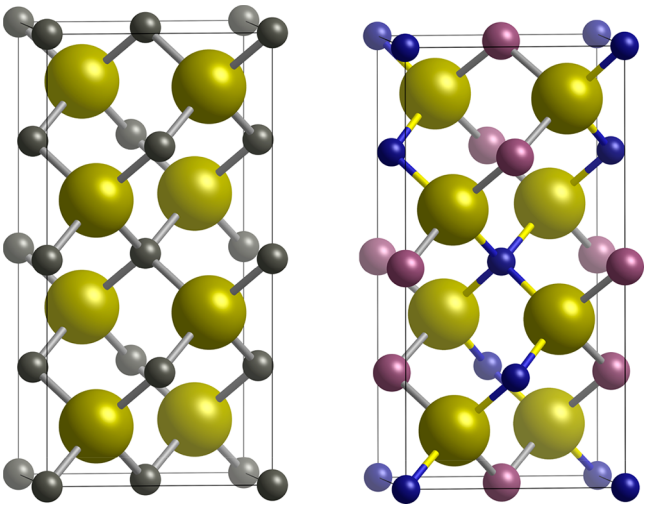

Figure 1. (Left) Two unit cells of cubic ZnS. (Right) One unit cell of $CuInS_2$.

22% probability of being occupied by a Zn atom. The ratio of ZnS to $CuInS_2$ incorporated during synthesis has been found[21,26,32] to not match the available mole ratios in the starting solution, since Zn^{2+} is kinetically incorporated at a lower rate.

In our curriculum we do this experiment in a nanochemistry course. The students have already been introduced to the idea of size-dependent properties of nanoscale materials, having previously prepared gold nanoparticles.[33] This synthesis serves as an introduction to QDs and further illustrates size-dependent properties. Our students are experienced in obtaining visible spectra, but most have not previously used a spectrofluorometer.

EXPERIMENTAL OVERVIEW

A combination of 0.0267 g (0.14 mmol) of CuI, 0.0409 g (0.14 mmol) of $In(CH_3COO)_3$, 0.0759 g (0.12 mmol) of $Zn(CH_3(CH_2)_{16}COO)_2$, 1 mL (4.2 mmol) of dodecanethiol, 0.23 mL (0.72 mmol) of oleic acid, and 16 mL of octadecene in a 25 mL Erlenmeyer flask is placed on a preheated 280 °C hot plate and stirred. Rapid heating is important. As the solution reaches 150 °C, all the materials dissolve. Heating for 15−20 min produces a metal sulfide (Scheme 1). The QD

Scheme 1. Dodecanethiolate Coordinates to the Metal Ion and Heating Decomposes the Metal Thiolate to Produce Some Metal Sulfide and Dodecylsulfide

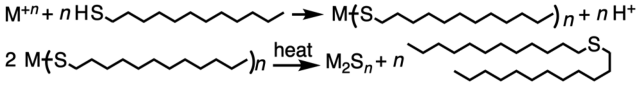

reaction then proceeds quickly with samples taken and quenched every 90 s or perhaps every 60 s if the color is changing noticeably (Figure 2). The quenched samples are stable at room temperature because a thiolate coating prevents their agglomeration (Figure 3). See the student directions and instructor notes in the Supporting Information for timing and further details.

It should be noted that this procedure starts with metal ions in their final oxidation state. There are related literature procedures[34] that use dodecanethiol to reduce Cu^{2+} to Cu^{+} rather than starting with Cu^{+}. QDs produced by that method often have less Cu^{+} than In^{3+} in the product, presumably accompanied by changes in S^{2-} for charge balance. Such defects can affect luminescence intensity.

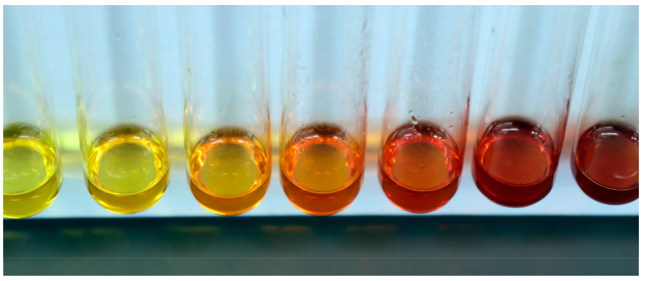

Figure 2. QD samples suspended in octadecene with reaction time increasing from left to right. Sequential samples differ in reaction time by 90 s. See Figure S1 for a larger range of samples.

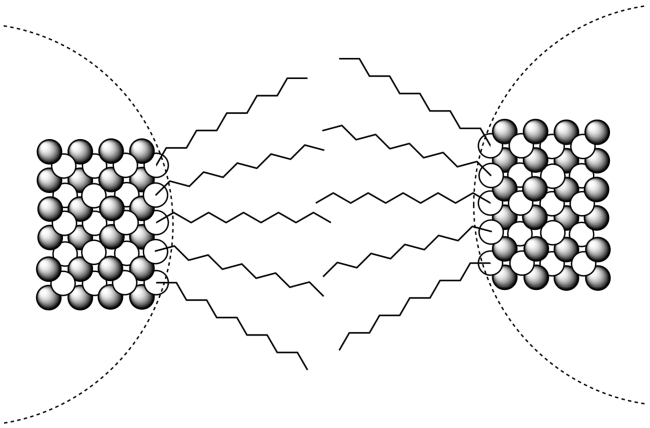

Figure 3. Incorporation of metal thiolate on the nanoparticle surface keeps the metal sulfide nanoparticles separated at room temperature. The dashed semicircle represents the surface of the metal sulfide nanoparticle. Light spheres represent sulfur atoms, and dark spheres represent metal atoms. See Figure 1 for the actual metal sulfide structure and stoichiometry. Hydrocarbons are shown in line notation.

Visible absorption spectra were taken using an Ocean Optics USB2000 and analyzed as shown in Figure 4 to find the band edge where the light has sufficient energy to excite an electron from the filled valence band to the empty conduction band.

Emission spectra were taken using a Horiba FluoroMax-4 spectrofluorometer with an excitation wavelength of 420 nm, slit widths of 5 nm, and recording at 1 nm steps. The starting octadecene, stearic acid, and oleic acid solution shows luminescence under these conditions to give a ∼490 nm peak which buries the luminescence from smaller QDs. As the reaction proceeds, the luminescent intensity and wavelength of the QDs increase. Useful information can be obtained for emission wavelengths >590 nm.

We find that if the temperature is below 190 °C, the reaction will take more than 3 h. If the temperature is above 230 °C, the reaction will occur too quickly to take samples. We suggest 210 °C where the heating plus sampling time takes about 40 min.

While we do not normally extend this experiment beyond a 3 h lab period, further characterization of the sample can be done after removal of the starting material and organic solvents. The QDs are extracted by repeated ethanol addition, centrifugation at 3500 rpm, and removal of the ethanol layer.

https://dx.doi.org/10.1021/acs.jchemed.9b00642
J. Chem. Educ. XXXX, XXX, XXX−XXX

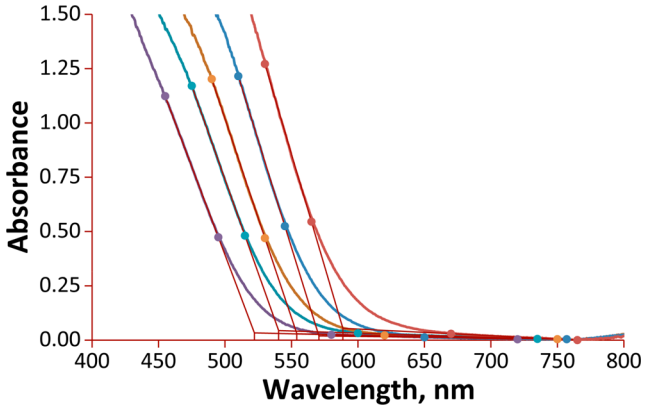

Figure 4. QD samples suspended in octadecene with reaction time increasing from left to right. Sequential samples differ in reaction time by 90 s. The absorption band edge is measured as the intersection of the extrapolated linear least-squares fits to all data between the circles for each segment.

For atomic absorption spectroscopy, the extracted sample was dissolved in heptane for transfer, evaporated, dissolved in a small amount of 70% nitric acid, and diluted to 100 mL with water, and 5 mL of that solution was diluted again to 25 mL. Standards were made using a solution containing both copper and zinc to compensate for potential interference. Atomic absorbance was measured at 324.7 and 213.0 nm for Cu and Zn, respectively, using an Agilent/Varian AA240FS instrument. Absorbance values were compared to a series of 0.2−2.5 ppm $Zn(CH_3COO)_2{\cdot}2H_2O$ and $CuSO_4{\cdot}5H_2O$ standards. For powder X-ray analysis, a separate synthesis was quenched all at once after 2 h of heating; the material was repeatedly extracted in ethanol, dissolved in heptane, and then evaporated onto a glass slide. For these small particles a step of 0.02° at 0.25°/min was used for the 25−60° 2θ scan with a Rigaku Miniflex II powder X-ray diffraction spectrometer. For infrared spectroscopy the extracted sample was evacuated for 2 days and then run neat using attenuated total reflectance sampling on a Nicolet iS10 FT-IR with diamond ATR.

HAZARDS

The reaction runs at a high temperature. The synthesis should be done in a fume hood. Dodecanethiol can cause skin burns and eye damage; it should not be inhaled and is toxic to aquatic life. Octadecene is flammable and will catch fire if spilled onto the hot plate. The pipet will be very hot and should be handled only by the bulb. Zinc, indium, and copper should not be ingested. The atomic absorption experiment uses concentrated nitric acid, which requires a fume hood and gloves.

RESULTS AND DISCUSION

After an initial induction period with little color change, the synthesis solution changes color from yellow to red as the particles grow (Figure 2). The band edge continuously varies from 420 to 680 nm (Figure 5) over the 40 min reaction as the particles get bigger. For longer reaction times, the solution becomes opaque which makes the absorbance hard to measure for longer wavelengths.

The photoluminescence peak wavelength increases with time once the particles become brighter than the starting material (Figure 6). Peak wavelengths lower than ∼590 nm appear as shoulders on an unchanging starting material emission peak at 490 nm.

This range of absorbance and emission colors could be from a $Zn_{2x}(CuIn)_{1-x}S_2$ solid solution series of ZnS and $CuInS_2$ with respective band gap wavelengths of 340 and 810 nm. To eliminate this possibility of spectral differences being due to different values of x, samples with different colors were examined by atomic absorption spectroscopy. The measured Zn/Cu ratio shows no correlation with band edge wavelength, indicating a constant composition product (Figure 7). The QD incorporated Zn/Cu ratio of the product was observed to be smaller than that of the reactants, and analysis of the ethanol wash from the sample purification showed an enhanced Zn/Cu ratio. Note that these analyses do not require weighing the samples before solution preparation. The technique measures the moles of Zn and of Cu, and the mole ratio is the quantity of interest. Assuming the moles of Cu^+ equal the moles of In^{3+}

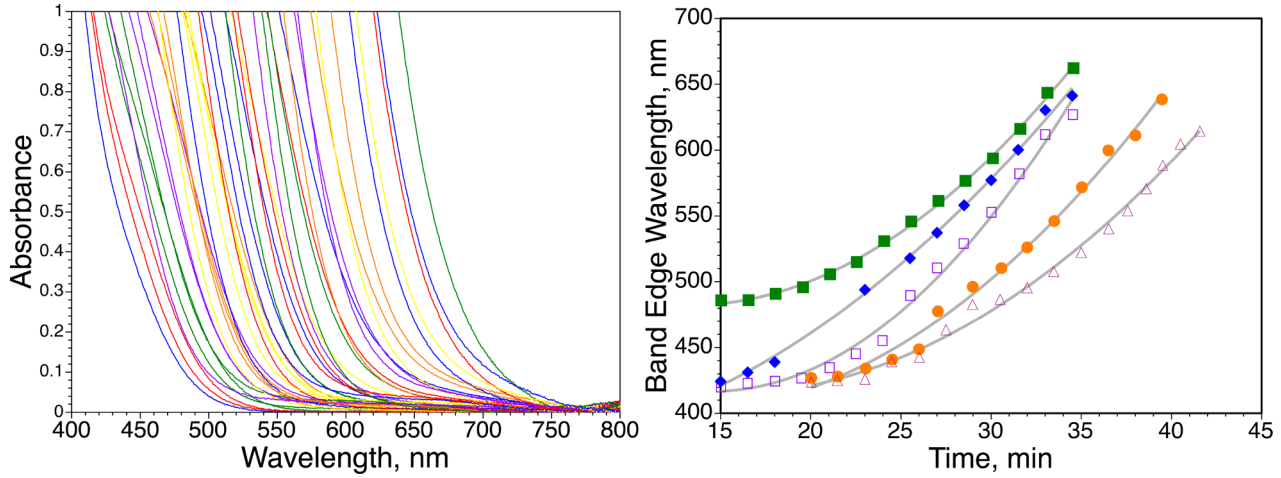

Figure 5. Baseline corrected visible absorption spectra. (Left) 43 samples from multiple experiments show a wide range of absorption band edges in the visible portion of the spectrum. Results are shown for a lab section. See Figure S2 for spectra obtained by one student. (Right) Five separate trials showing variation in band edge as reaction time increases, measured as in Figure 4. Most trials show an initial induction period with very little change at the beginning, but once the reaction occurs the wavelength increases quickly. The fit lines are only meant to guide your eye. The same symbols are used for the same solutions in Figure 6.

https://dx.doi.org/10.1021/acs.jchemed.9b00642
J. Chem. Educ. XXXX, XXX, XXX−XXX

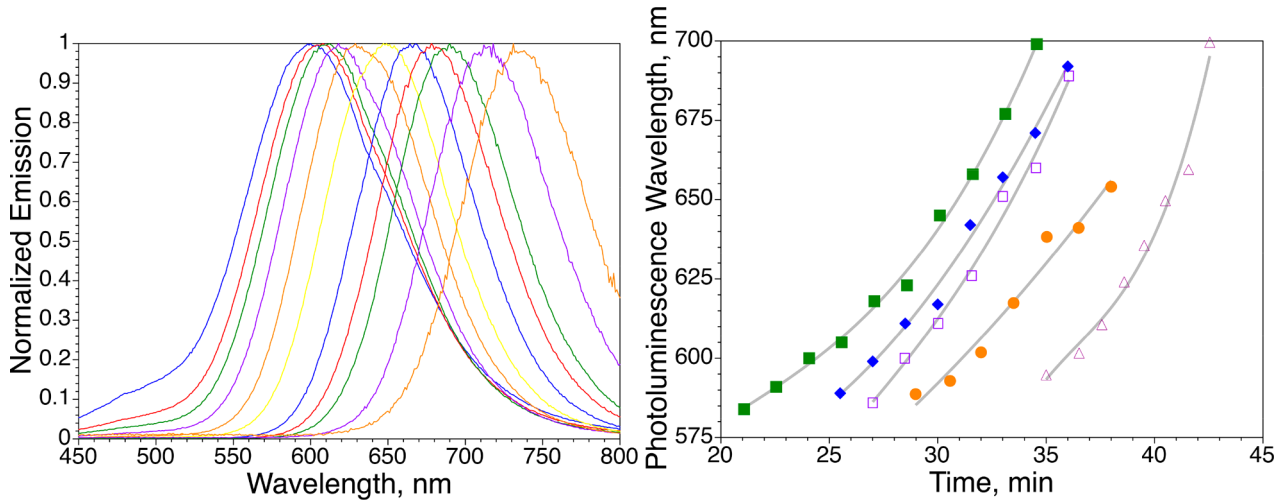

Figure 6. (Left) Normalized emission spectra from one series of QDs excited at 420 nm. Longer reaction times correspond with longer peak wavelengths. Sequential samples differ in reaction time by 90 s. (Right) Photoluminescence wavelength peaks from five different trials increase as time increases. Lower wavelength peaks are masked by luminescence of the reactants. The fit lines are only meant to guide your eye. The same symbols are used for the same solutions in Figure 5.

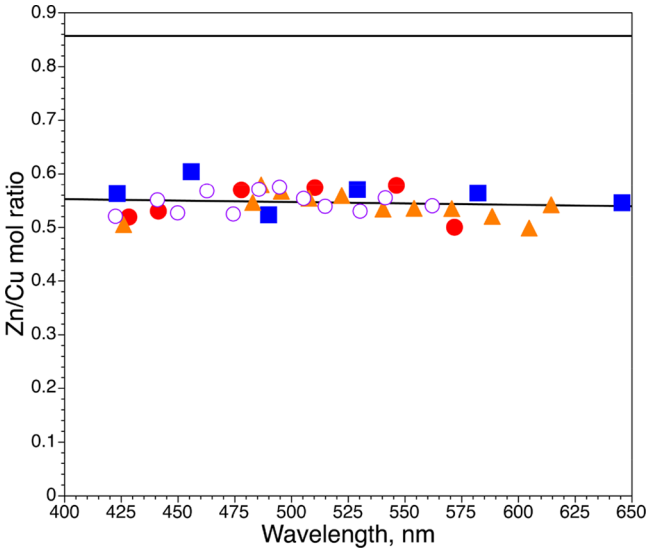

Figure 7. Mole ratio of Zn/Cu in the products after washing. The atomic absorption data of 36 samples from 4 separate series is plotted as a function of the absorption band edge of each of those solutions. *There is no correlation between the unchanging chemical composition and the changing absorption band edge.* The upper line indicates the 0.86 Zn/Cu mol ratio in the starting materials. For the series represented by the open circles, analysis of the sample purification wash showed an average 4 Zn/Cu. Assuming the general formula is $Zn_{2x}(CuIn)_{1-x}S_2$, the observed Zn/Cu ratio in the samples corresponds to $x = 0.22$.

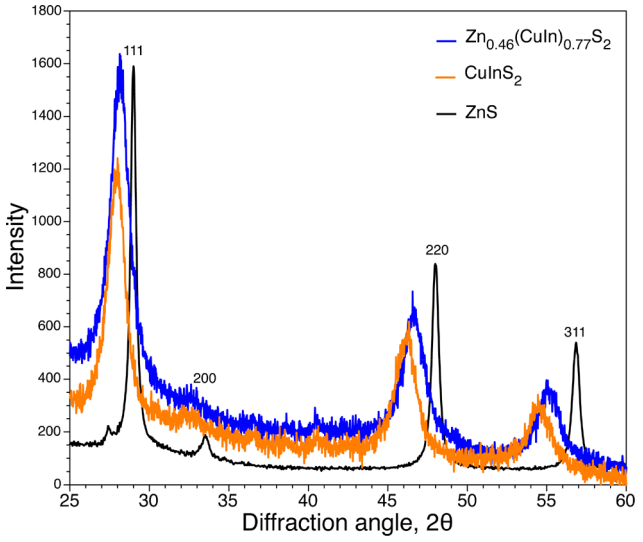

Figure 8. XRD of $CuInS_2$, $Zn_{0.46}Cu_{0.77}In_{0.77}S_2$, and ZnS deposited on a glass substrate. All three are cubic or pseudocubic structures. Miller indexes of the zinc blende structure are labeled. The $CuInS_2$ sample was prepared by the same procedure used to synthesize $Zn_{0.46}Cu_{0.77}In_{0.77}S_2$ but without the addition of any Zn starting material. Bulk ZnS was supplied by ProChem.

as required by charge balance, then $x = 0.22$ in $Zn_{2x}(CuIn)_{1-x}S_2$, and the QDs synthesized by this procedure have the formula $Zn_{0.44}(CuIn)_{0.78}S_2$.

If the change in color as the reaction proceeds is not due to a change in composition, then a possible explanation is a quantum size effect of the nanoparticles; i.e., these materials are QDs. As a confirmation of the composition, an entire batch was analyzed by X-ray powder diffraction (XRD) and compared with scans of ZnS and $CuInS_2$ using the same sampling method on the same instrument with the same scan conditions (Figure 8). If Vegard's rule that solid solutions exhibit weighted average lattice parameters holds, and assuming the formula is $Zn_{2x}(CuIn)_{1-x}S_2$, then $x = 0.23$ which is in agreement with our atomic absorption results that $x = 0.22$. Our measured lattice parameter of 5.50 Å is in reasonable agreement with the 5.48 Å reported[31] for the product from a solid-state 950 °C synthesis with $x = 0.225$.

The infrared spectrum of the extracted QDs matches that of dodecanethiol (Figure 9) and does not match that of octadecene, stearic acid, or oleic acid. This is consistent with the presence of dodecanethiolate as a surface ligand.

The effective mass model[3,5,3,4,6,7,9,10] suggests

$$E_g^{nano} = E_g^{bulk} + \frac{h^2}{8m_0r^2}\left(\frac{1}{m_e^*} + \frac{1}{m_h^*}\right) - \frac{1.8e^2}{4\pi\varepsilon\varepsilon_o r}$$

https://dx.doi.org/10.1021/acs.jchemed.9b00642
J. Chem. Educ. XXXX, XXX, XXX−XXX

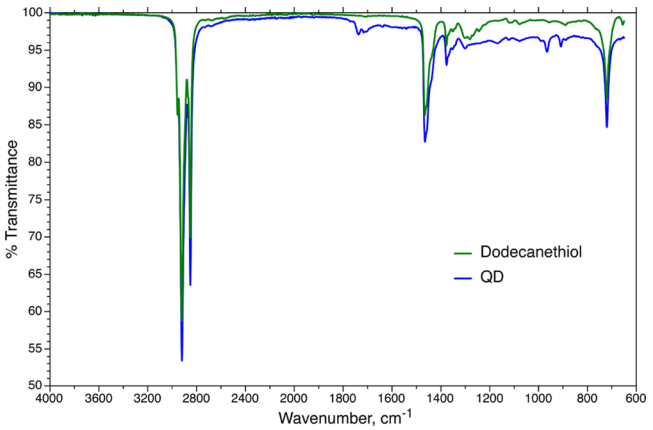

Figure 9. IR spectra of dodecanethiol and of extracted QDs after 48 h under vacuum. The similarity of these two spectra suggests that the QDs are coated with dodecanethiolate.

where $E_g = hc/\lambda$, r is the radius of the nanoparticle, and the constants and values[36] for $CuInS_2$ are given in Box 1. The

Box 1

Constants

- $h = 6.626 \times 10^{-34}$ J s
- $c = 2.998 \times 10^{8}$ m/s
- $e = 1.602 \times 10^{-19}$ C
- $\varepsilon_0 = 8.854 \times 10^{-12}$ $C^2/N/m^2$
- $m_0 = 9.110 \times 10^{-31}$ kg

Values for $CuInS_2$

- $\lambda^{bulk} = 810$ nm
- $m_e^* = 0.16$, relative mass of conduction band e^-
- $m_h^* = 1.3$, relative mass of valence band hole
- $\varepsilon = 11$, relative permittivity

second term is the particle-in-a-box confinement energy for an electron−hole pair in a spherical QD, and the third term is the Coulomb attraction between an electron and hole modified by the screening of charges by the crystal. After multiplying by r^2 and rearranging, the quadratic formula to find r gives

$$r = \frac{-\left(\frac{1.8e^2}{4\pi\varepsilon\varepsilon_0}\right) + \sqrt{\left(\frac{1.8e^2}{4\pi\varepsilon\varepsilon_0}\right)^2 + (E_g^{nano} - E_g^{bulk})\frac{h^2}{2m_0}\left(\frac{1}{m_e^*} + \frac{1}{m_h^*}\right)}}{2(E_g^{nano} - E_g^{bulk})}$$

When this equation is used for $CuInS_2$ the predicted particle diameters for visible spectrum band edge wavelengths are in the 3−6 nm range. This is in agreement with sizes reported from transmission electron microscope measurements using related syntheses.[17,21,25,32]

STUDENT LEARNING

To show that all the samples have the same composition, we provide Figure 7 rather than adding a lab period to have students collect this data. We find that students clearly understand that these nanoparticles are getting larger as the reaction proceeds and that the property changes are due to this change in size.

Students did not have difficulty deciding that the charge on the QD is neutral if they correctly identified the oxidation states of Zn^{2+}, Cu^{+}, and In^{3+}.

When students used rulers to extrapolate and find the absorption band edge data there were large variations in results, even between lab partners measuring the same spectra. We now use an Excel template[37] (Figure 4) to pick linear segments that are least-squares fit and the intersection calculated.

Students did have considerable trouble working out the units in the effective mass model to predict the particle sizes.

It is often necessary to have a class discussion about usable spectroscopy data ranges. Opaque solutions with really large particles do not give good absorption data. The really small particles do not luminesce well enough to mask the starting materials so it can appear that the luminescence wavelength is not changing at first. For the optional atomic absorption analysis the working range for the calibration curve only covers an order of magnitude. Fortunately, all the samples have the same composition so the small working range is not a problem. Student evaluations suggest they find the extractions and subsequent atomic absorption analysis tedious, especially since the results show all their samples are the same. We no longer do the atomic absorption analysis in class.

Understanding and explaining evidence for this experiment showing band gap excitation instead of molecular absorbance was a concept students found difficult to grasp, but the broad excitation profile (anything bigger than the band gap will excite electrons) and the change in color (molecules would not change size as do the nanoparticles with continued reaction) are fundamental concepts worth the struggle.

SUMMARY

The analysis data indicates these samples are $Zn_{0.44}(CuIn)_{0.78}S_2$ quantum dots, with a constant composition but different colors. The predicted diameters for the measured energies are below 6 nm. This experiment provides a visible example of size-dependent properties in the nanoscale and is done without Cd, making this a greener and safer synthesis, although it does still involve using a hot flammable solvent and require a fume hood.

ASSOCIATED CONTENT

Supporting Information

The Supporting Information is available at https://pubs.acs.org/doi/10.1021/acs.jchemed.9b00642.

Experimental protocol including student directions and laboratory questions (PDF, DOCX)

Instructor notes and answer key (PDF, DOCX)

Additional supporting figures (PDF, DOCX)

AUTHOR INFORMATION

Corresponding Author

George Lisensky − *Beloit College, Beloit, Wisconsin 53511, United States;* orcid.org/0000-0002-1000-406X; Email: lisensky@beloit.edu

Other Authors

Ross McFarland-Porter − *Beloit College, Beloit, Wisconsin 53511, United States*

Weltha Paquin − *Beloit College, Beloit, Wisconsin 53511, United States*

Kangying Liu − *Beloit College, Beloit, Wisconsin 53511, United States*

https://dx.doi.org/10.1021/acs.jchemed.9b00642
J. Chem. Educ. XXXX, XXX, XXX−XXX

Complete contact information is available at:
https://pubs.acs.org/10.1021/acs.jchemed.9b00642

Notes

The authors declare no competing financial interest.

■ ACKNOWLEDGMENTS

The authors gratefully acknowledge the Beloit College Sanger Summer Scholars Program (2016) and Norris research funds (2019); partial support of this research by NSF through the University of Wisconsin Materials Research Science and Engineering Center (DMR- 1720415); and the 2017, 2018, and 2019 Beloit College nanochemistry classes for helping refine this experiment.

■ REFERENCES

(1) Boatman, E. M.; Lisensky, G. C.; Nordell, K. J. A Safer, Easier, Faster Synthesis for CdSe Quantum Dot Nanocrystals. *J. Chem. Educ.* **2005**, *82*, 1697−1699.
(2) Landry, M. L.; Morrell, T. E.; Karagounis, T. K.; Hsia, C. H.; Wang, C. Y. Simple Syntheses of CdSe Quantum Dots. *J. Chem. Educ.* **2014**, *91* (2), 274−279.
(3) Bauer, C. A.; Hamada, T. Y.; Kim, H.; Johnson, M. R.; Voegtle, M. J.; Emrick, M. S. An Integrated, Multipart Experiment: Synthesis, Characterization, and Application of CdS and CdSe Quantum Dots as Sensitizers in Solar Cells. *J. Chem. Educ.* **2018**, *95* (7), 1179−1186.
(4) Harris, C.; Gaster, C.; Gelabert, M. C. Reverse Micelles as Templates for the Fabrication of Size-Controlled Nanoparticles: A Physical Chemistry Experiment. *J. Chem. Educ.* **2019**, *96* (3), 565−570.
(5) Kippeny, T.; Swafford, L. A.; Rosenthal, S. J. Semiconductor Nanocrystals: A Powerful Visual Aid for Introducing the Particle in a Box. *J. Chem. Educ.* **2002**, *79*, 1094−1100.
(6) Nedelijković, J. M.; Patel, R. C.; Kaufman, P.; Joyce-Pruden, C.; O'Leary, N. Synthesis and optical properties of quantum-sized metal sulfide particles in aqueous solution. *J. Chem. Educ.* **1993**, *70*, 342−345.
(7) Winkler, L. D.; Arceo, J. F.; Hughes, W. C.; DeGraff, B. A.; Augustine, B. H. Quantum dots: an Experiment for Physical or Materials Chemistry. *J. Chem. Educ.* **2005**, *82* (11), 1700.
(8) Winkelmann, K.; Noviello, T.; Brooks, S. Preparation of CdS Nanoparticles by First-Year Undergraduates. *J. Chem. Educ.* **2007**, *84*, 709−710.
(9) Hale, P. S.; Maddox, L. M.; Shapter, J. G.; Voelcker, N. H.; Ford, M. J.; Waclawik, E. R. Growth Kinetics and Modeling of ZnO Nanoparticles. *J. Chem. Educ.* **2005**, *82*, 775−778.
(10) Reid, P. J.; Fujimoto, B.; Gamelin, D. R. A Simple ZnO Nanocrystal Synthesis Illustrating Three-Dimensional Quantum Confinement. *J. Chem. Educ.* **2014**, *91* (2), 280−282.
(11) Pham, S. N.; Kuether, J. E.; Gallagher, M. J.; Hernandez, R. T.; Williams, D. N.; Zhi, B.; Mensch, A. C.; Hamers, R. J.; Rosenzweig, Z.; Fairbrother, H.; Krause, M. O. P.; Feng, Z. V.; Haynes, C. L. Carbon Dots: A Modular Activity To Teach Fluorescence and Nanotechnology at Multiple Levels. *J. Chem. Educ.* **2017**, *94* (8), 1143−1149.
(12) Schneider, E. M.; Bartsch, A.; Stark, W. J.; Grass, R. N. Safe One-Pot Synthesis of Fluorescent Carbon Quantum Dots from Lemon Juice for a Hands-On Experience of Nanotechnology. *J. Chem. Educ.* **2019**, *96* (3), 540−545.
(13) Pan, Y.; Li, Y. R.; Zhao, Y.; Akins, D. L. Synthesis and Characterization of Quantum Dots: A Case Study Using PbS. *J. Chem. Educ.* **2015**, *92* (11), 1860−1865.
(14) Markina, N. E.; Pozharov, M. V.; Markin, A. V. Synthesis of Copper(I) Oxide Particles with Variable Color: Demonstrating Size-Dependent Optical Properties for High School Students. *J. Chem. Educ.* **2016**, *93* (4), 704−707.
(15) Shekhirev, M.; Goza, J.; Teeter, J. D.; Lipatov, A.; Sinitskii, A. Synthesis of Cesium Lead Halide Perovskite Quantum Dots. *J. Chem. Educ.* **2017**, *94* (7), 1150−1156.
(16) Liu, Y.; Huang, F.; Xie, Y.; Cui, H.; Zhao, W.; Yang, C.; Dai, N. Controllable Synthesis of $Cu_2In_2ZnS_5$Nano/Microcrystals and Hierarchical Films and Applications in Dye-Sensitized Solar Cells. *J. Phys. Chem. C* **2013**, *117*, 10296−10301.
(17) Yue, L.; Rao, H.; Du, J.; Pan, Z.; Yu, Y.; Zhong, X. Comparative advantages of Zn−Cu−In−S alloy QDs in the construction of quantum dot-sensitized solar cells. *RSC Adv.* **2018**, *8*, 3637−3645.
(18) Villas-Boas, A. Samsung just unveiled the widest computer monitor you can buy − here's how it looks in person. *Business Insider* https://www.businessinsider.com/samsung-qh90-super-ultra-wide-329-monitor-photos-2017-6 (accessed December 2019).
(19) Regulacio, M. D.; Han, M. Y. Multinary I-III-VI_2 and I_2-II-IV-VI_4 Semiconductor Nanostructures for Photocatalytic Applications. *Acc. Chem. Res.* **2016**, *49*, 511−519.
(20) Song, W. S.; Yang, H. Efficient White-Light-Emitting Diodes Fabricated from Highly Fluorescent Copper Indium Sulfide Core/Shell Quantum Dots. *Chem. Mater.* **2012**, *24*, 1961−1967.
(21) Guo, W.; Chen, N.; Dong, C.; Tu, Y.; Chang, J.; Zhang, B. One-Pot Synthesis of Hydrophilic ZnCuInS/ZnS Quantum Dots for *in vivo* Imaging. *RSC Adv.* **2013**, *3*, 9470−9475.
(22) Odularu, A. T. Metal Nanoparticles: Thermal Decomposition, Biomedicinal Applications to Cancer Treatment, and Future Perspectives. *Bioinorg. Chem. Appl.* **2018**, *2018*, 9354708.
(23) Occupational Safety and Health Administration, United States Department of Labor, Cadmium, https://www.osha.gov/SLTC/cadmium, and Lead, https://www.osha.gov/SLTC/lead/ (accessed December 2019).
(24) Shen, S.; Zhang, Y.; Peng, L.; Xu, B.; Du, Y.; Deng, M.; Xu, H.; Wang, Q. Generalized synthesis of metal sulfide nanocrystals from single-source precursors: size, shape and chemical composition control of their properties. *CrystEngComm* **2011**, *13*, 4572−4579.
(25) Chetty, S. S.; Praneetha, S.; Basu, S.; Sachidanandan, C.; Murugan, A. V. Sustainable, Rapid Synthesis of Bright-Luminescent $CuInS_2$-ZnS Alloyed Nanocrystals: Multistage Nano-xenotoxicity Assessment and Intravital Fluorescence Bioimaging in Zebrafish-Embryos. *Sci. Rep.* **2016**, *6*, 26078.
(26) Fu, M.; Luan, W.; Tu, S. T.; Mleczko, L. Green synthesis of $CuInS_2$/ZnS Nanocrystals with High Photoluminescence and Stability. *J. Nanomater.* **2015**, *2015*, 842365.
(27) Vahidshad, Y.; Ghasemzadeh, R.; Irajizad, A.; Mirkazemi, S. M. Synthesis and Characterization of Copper Indium Sulfide Chalcopyrite Structure with Hot Injection Method. *J. Nanostructures* **2013**, *3*, 145−154.
(28) van Embden, J.; Chesman, A. S. R.; Jasieniak, J. J. The heat-up synthesis of colloidal nanocrystals. *Chem. Mater.* **2015**, *27*, 2246−2285.
(29) Chi, T. T. K.; Thuy, U. T. D.; Huyen, T. T. T.; Thuy, N. T. M.; Le, N. T.; Liem, N. Q. Enhanced Optical Properties of Cu-In-S Quantum Dots with Zn Addition. *J. Electron. Mater.* **2016**, *45* (5), 2449−2454.
(30) Gromova, M.; Lefrançois, A.; Vaure, L.; Agnese, F.; Aldakov, D.; Maurice, A.; Djurado, D.; Lebrun, C.; de Geyer, A.; Schülli, T. U.; Pouget, S.; Reiss, P. Growth Mechanism and Surface State of $CuInS_2$ Nanocrystals Synthesized with Dodecanethiol. *J. Am. Chem. Soc.* **2017**, *139*, 15748−15759.
(31) Schorr, S.; Tovar, M.; Sheptyakov, D.; Keller, L.; Geandier, G. Crystal Structure and Cation Distribution in the Solid Solution Series 2(ZnX)-$CuInX_2$ (X = S, Se Te). *J. Phys. Chem. Solids* **2005**, *66*, 1961−1965.
(32) Wagner, G.; Fleischer, F.; Schorr, S. Extension of the two-phase field in the system $2(ZnS)_x(CuInS_2)_{1-x}$ and structural relationship between the tetragonal and cubic phase. *J. Cryst. Growth* **2005**, *283*, 356−366.
(33) McFarland, A. D.; Haynes, C. L.; Mirkin, C. A.; Van Duyne, R. P.; Godwin, H. A. Color My Nanoworld. *J. Chem. Educ.* **2004**, *81* (4), 544A−544B.

(34) Liu, S.; Xu, H.; Nie, L.; Ren, Y.; Yuan, R. Spray pyrolysis deposition of Cu-Zn-In-S solid-solution thin films with tunable compositions and band gaps. *Mater. Sci. Semicond. Process.* **2015**, *40*, 20−25.
(35) Brus, L. Electronic wave functions in semiconductor clusters: experiment and theory. *J. Phys. Chem.* **1986**, *90* (12), 2555−2560.
(36) Shay, J. L.; Tell, B.; Kasper, H. M.; Schiavone, L. M. $p - d$ Hybridization of Valence Bands of I-III-$\mathbf{VI}_2$ Compounds. *Phys. Rev. B* **1972**, *5*, 5003−5005.
(37) An Excel template is used to extrapolate the user-selected linear portions of the absorbance as a function of wavelength graph to find the band edge. Upon opening, Excel will give a macro warning because this sheet uses macros to make plots. Lisensky, G.; Band Edge Spreadsheet. https://chem.beloit.edu/classes/excel/baseline_intersect.xlsm (accessed December 2019).

https://dx.doi.org/10.1021/acs.jchemed.9b00642
J. Chem. Educ. XXXX, XXX, XXX−XXX